Self-assembly of the non-planar Fe(III) phthalocyanine small-molecule: unraveling the impact on the magnetic properties of organic nanowires

A. Nicolas Filippin,[1] Victor Lopez-Flores,[1] T. Cristina Rojas,[1] Zineb Saghi,[2,3] Victor J. Rico,[1] Juan R. Sanchez-Valencia,[1] Juan P. Espinos,[1] Andrea Zitolo,[4] Michel Viret,[5] Paul A. Midgley,[2] Angel Barranco,[1] Ana Borras[1]**

1 Nanotechnology on Surfaces Laboratory, Instituto de Ciencia de Materiales de Sevilla, CSIC-Universidad de Sevilla, c/Américo Vespucio 49, 41092 Sevilla (Spain)

2 Department of Materials Science and Metallurgy, University of Cambridge, 27 Charles Babbage Road, CB3 0FS, Cambridge (United Kingdom)

3 University of Grenoble Alpes, Grenoble F-38000; CEA, LETI, MINATEC Campus, Grenoble F- 38054 (France)

4 Synchrotron SOLEIL, L'Orme des Merisiers, BP 48 Saint Aubin, Gif-sur-Yvette (France)

5 Service de Physique de l'État Condensé (CNRS URA 2464), CEA Saclay, Gif-sur-Yvette 91190 (France)

ABSTRACT. In this article we show for the first time the formation of magnetic supported organic nanowires (ONWs) driven by self-assembly of a non-planar Fe(III) phthalocyanine chloride (FePcCl) molecule. The ONWs grow by a crystallization mechanism on roughness-tailored substrates. The growth methodology consists in a vapor deposition under low vacuum and mild temperature conditions. The structure, microstructure and chemical composition of the FePcCl NWs are thoroughly elucidated and compared with those of Fe(II) phthalocyanine NWs by a consistent and complementary combination of advanced electron microscopies and X-ray spectroscopies. In a further step, we follow to vertically align of the NWs by conformal deposition of a SiO_2 shell. Such orientation is critical to analyze the magnetic properties of the FePcCl and FePc supported NWs. A ferromagnetic behavior below 30K with an easy axis perpendicular to the phthalocyanine plane was observed in the two cases with the FePcCl nanowires presenting a wider hysteresis. These results open the path to the fabrication of nanostructured one-dimensional small-molecule spintronic devices.

Tailoring materials structure at the nanoscale has prompted the research on new and exciting properties over the last two decades. This is particularly true on one-dimensional (1D) nanostructures (nanotubes, nanowires, nanorods or nanobelts) with longitudinal sizes orders of magnitude larger than the cross-sectional sizes.[1] Among them, organic nanowires (ONW) form a family of nanostructures with remarkable optic, electronic, sensing and wetting properties.[2-12] In addition, the development of ONWs devices offers potential for low cost and flexible devices and versatility through the molecular design of their building blocks. The methods for the synthesis of these 1D systems generally relay on three approaches including template procedures, solution-phase deposition and vapour transport.[2-4,6,10,13] Condensation from vapour phase at low pressure (or simply physical vapour deposition, PVD) counts within the last group

and presents interesting features such as: i) direct formation of single crystal nanowires with controlled morphology on different substrates; ii) highly adaptable to a large amount of different π-conjugated small molecules; iii) high growth rate and controlled density of nanowires with appropriated homogeneity; iv) solventless and one-step; and, v) straightforward compatibility with other vacuum deposition and processing methods.[2,14-18] The method consists in the low-pressure sublimation of purely organic or metalorganic small-molecules from the bulk crystals counterpart and their condensation on the surface of diverse supports. These molecules self-assemble into supported single-crystal nanowires of tens of nanometres width and several microns length.[14,15,18] Such heterogeneous crystallization process can be enhanced by including nucleation centres at the substrate to trigger the preferential condensation of molecules on those spots.[14,15] Formation of ONWs has been reported during the last years on an ample variety of surfaces including metal and metal oxide thin films and organic supports.[12,14,18-21] The main parameter conditioning the growth of ONWs is the morphology of the surface instead of its chemical nature. Thus, the surfaces suitable for the growth of a high density of nanowires usually present a certain roughness produced for instance by the distribution of metal or metal oxide nanoparticles on a flat substrate or simply by the nanostructured thin film surfaces features. On the other hand, the preferential self-assembly in the direction of the nanowire length is driven by the π-π stacking of conjugated organic molecules. The most studied single-crystalline nanowires grown by vapour-phase condensation are formed by extended aromatic molecules including also heteroatoms and metalorganic molecules (for instance, perylene bisimides, (metal)-porphyrins and (metal)-phthalocyanines).[2,6,7,14-16] The role played by the heteroatoms and side chain modifications in purely organic molecules as well as metal cations within metal porphyrins and phthalocyanines is critical in the properties of the functional molecules and thereof in the

applications of the ONWs. During the last years, numerous articles have reported on the molecular design attending to the side chain modification to improve solubility and to develop ONWs with ad hoc properties. Thorough analyses on the electrical and optical properties of metal-porphyrins and metal-phthalocyanines as a function of the metal cation have been published.[2,4] Thus, planar aromatic backbone molecular structures are extensively exploited as building blocks of small-molecule single crystal nanowires, meanwhile, there is a lack of information in the bibliography regarding the formation/assembling of similar structures from non-planar conjugated molecules. The structure and symmetry of the phthalocyanines depend on their composition. Metal free phthalocyanines H_2Pc (D_{2h}) and metal-phthalocyanines of the most common light divalent transition cations MPc (D_{4h}) are planar conjugated systems. In the case of metal-phthalocyanines of trivalent cations, the resulting molecules are non-planar (C_{4v}) with an out-of-plane anionic species compensating the extra charge. On the other hand, phthalocyanine molecules present interesting magnetic properties recently unraveled for monolayers of metal-phthalocyanines adsorbed on substrates or forming thin films,[22-26] as ultrathin films on semiconductors,[24] and as superconducting self-assembled structures on epitaxial films.[25]

In this work, we report the synthesis, microstructure and magnetic properties of ONWs made of Fe(III) phthalocyanine chloride (FePcCl) and Fe(II) phthalocyanine (FePc). The choice of these molecules was not arbitrary. FePc (see schematics on Figure 1) holds an Fe(II) ion with an unbalanced spin of S = 1.[26] This molecule presents interesting magnetic properties when π-π stacked in crystalline thin films[23,29] but has not yet been studied from this point of view forming 1D nanostructures. The scarcely studied FePcCl molecule is quite similar, but with a Cl atom standing out of the phthalocyanine plane, in line with the central Fe(III) ion (see Figure 1). This ion holds a larger unbalanced spin S = 5/2, which would, in principle, enhance the exchange

coupling between molecules. However, as we will show below, the introduction of the Cl atom leads to a modification of the out-of-plane interaction providing a significantly difference in the magnetic properties. Furthermore, it has been reported[26] that molecules similar to FePcCl tend to lose the Cl atom when deposited onto conductive substrates, with a partial reduction of the Fe(III) ion to Fe(II), effectively transforming the FePcCl molecule into FePc.

As far as we know, this is the first time that a protocol for the formation of supported nanowires from non-planar phthalocyanines is presented. A detailed characterization applying High Resolution Transmission Electron Microscopy (HREM), Selected Area Electron Diffraction (SAED), Scanning Transmission Electron Microscopy (ESEM), Energy-Dispersive X-ray spectroscopy (EDX), X-ray Absorption Spectroscopy (XANES/EXAFS) and X-ray Photoemission Spectroscopy (XPS) aimed a thorough elucidation of the structure and composition of the ONWs. In addition, following a protocol recently developed[19,21,28] we show the vertical alignment of the as-grown FePc and FePcCl ONWs after deposition of a conformal SiO_2 shell by plasma enhanced chemical vapour deposition (PECVD). Both the effect of the Fe(III) cation presence along the NWs structure and their vertical alignment will be addressed regarding their magnetic properties.

Results and discussion

Figure 1a) shows the planar view of a FePc nanowire array grown on a Si(100) substrate decorated with an aluminium nanostructured film (see Methods for experimental details). Similarly to previous results,[14-16] the nanowires grow from the interface with the substrate by a crystallization processes initiated at a metallic nanoparticle decorated surface. They are consistently formed in rectangular shapes that are constant through their lengths, with cross

sections mean value ~ 57 nm (NWs thickness in the range between 19 and 118 nm) and lengths over 1-2 μm. Figure S1 shows the histograms obtained after statistics in more than 150 NWs obtained after image analyses of several SEM micrographs. The nanowires distribution covers random directions with respect to the substrate surface in a high density over 15 ONWs/μm^2. Figure 1 b) presents the nanowire array obtained from FePcCl molecules following the optimized experimental protocol on a Al/Si(100) substrate. At first sight, the results indicates the non-planar phthalocyanine also self-assembles forming supported nanowires with a similar rectangular shape, but with a higher density that in the case of the FePc. The FePcCl nanowires mean length (~1-2 μm) is similar to that of the FePc nanowires (see the pictures on the right side in Figures 1a and 1b). However, the average cross section is thinner, ~ 53 nm (NWs thickness in the range between 19 and 98 nm).

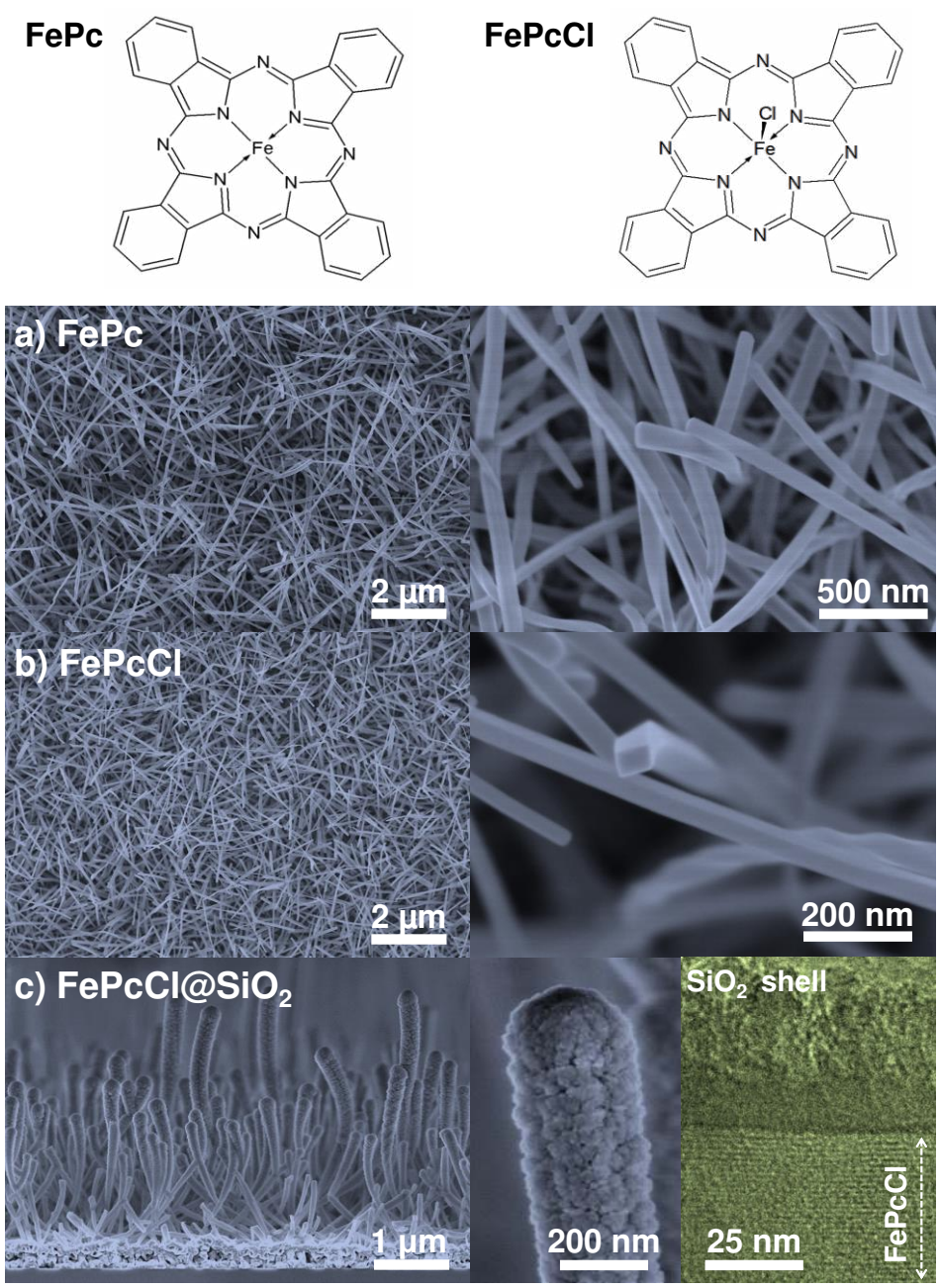

Figure 1. Normal view SEM micrographs of FePc (a) and FePcCl (b) nanowires grown on Al/Si(100) substrates. c) Cross-sectional view of the FePcCl@SiO_2 nanowires (left), higher magnification image showing the globular microstructure of the SiO_2 shell (center) and HREM image of the core@shell nanostructure (right). The top panel shows the chemical structure of the nanowires precursor molecules FePc and FePcCl.

The combination of High-Resolution Electron Microscopy (HREM) and Selected Area Electron Diffraction (SAED) provides the structural characterization of individual nanowires. Figure 2 a-b) show the HREM micrographs of single nanowires of the planar (FePc) and non-planar (FePcCl) phthalocyanines. This magnification allows distinguishing the vertical columns of the single crystals and determining the inter-planar distance. The measured inter-columnar distances were 1.30 ± 0.05 nm and 1.32 ± 0.05 nm, for FePc and FePcCl respectively. These values were confirmed by the respective 2D Fourier transforms (see the insets in the figures). However, the resolution of the TEM is not enough to distinguish between two layers of the stack in the real space. By recording the SAED diagrams of the two samples at the (001) zone (Figure 2 c-d), we were able to see a set of diffraction dots indexed as the repeating column direction (100) and the inter-plane stacking direction (010). FePc nanowires yield distances of d(100) = 1.30 nm and d(010) = 0.40 nm, while for the FePcCl nanowire, d(100) = 1.32 nm and d(010) = 0.46 nm. Note that such difference in the interplanar stacking is in good agreement with the Cl ionic radius (i.e., 0.175 nm)[29] as shown in the Schematic S1 in the Supporting Information Section. The interplanar stacking direction of the FePc nanowire forms an angle of 85º respect to the intercolumnar direction, which means that the vertical stacking is slightly skewed from the perpendicular to the columns. This arrangement is characteristic of the phthalocyanines' triclinic crystal structure.[14,15,30,31] Furthermore, in the FePc SAED diagram we appreciate an intensity increase of the diffraction dots corresponding approximately to the (210) direction and also a minor one on the (310) direction. These effects could be attributed to the herringbone angle of the molecular arrangement which would be oriented to this direction (i.e., between 20º (210) and 28º (310) from the inter-column direction).[15] A similar case occurs in the FePcCl SAED diagram, where the interplanar stacking direction is at 87º from the intercolumnar direction. In

this case, the diffraction intensity increase is located between the (100) and the (200) (i.e., between 15º and 20º), presenting approximately a similar increase in both cases. Figure 2 c-d) also shows the 2D Fourier Transform of the corresponding triclinic herringbone models with the calculated distances, angles and orientation of the molecules (see the models in the corresponding insets and Schematic S1). Note that, although there is always some degree of amorphisation of the nanowire crystalline structure under the electron beam during the image acquisition, these models corresponds fairly well with the experimental SAED diagrams. In addition, these results for individual nanowires structure agree with the microstructural characterization carried out of NWs-arrays by X-ray Diffraction at grazing angles (Supporting Information Section S1). GAXRD diagrams in the SI show diffraction peaks corresponding to both the nanowire samples and to the substrates (Cu and Cu_2O nanostructured films), depicting three clearly defined peaks at the lowest angles corresponding to the (200), (202) and (402) planes.[32]

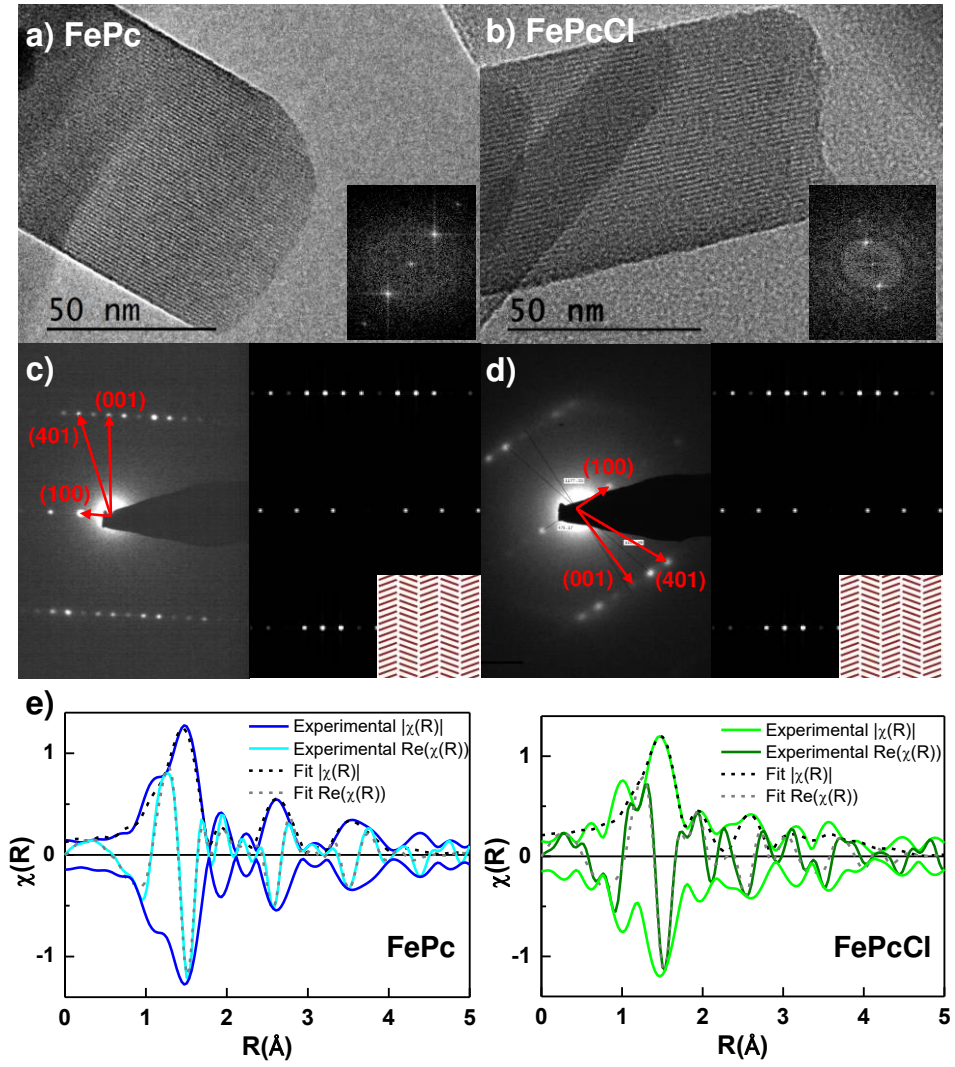

Figure 2. HREM micrographs of single-crystalline nanowires of (a) FePc and (b) FePcCl. The respective insets are the corresponding 2D Fourier transforms. SAED diagrams and calculated diffraction diagrams (right) of (c) FePc and (d) FePcCl nanowires. The insets show the herringbone structures for each composition. (e) EXAFS signals Fourier Transforms (imaginary part and magnitude) from the samples with their corresponding fits.

At higher angles, a set of four peaks corresponding to (111), (112), (312) and (313) planes appear as well for both samples. The last two peaks correspond to the (111) planes of the Cu_2O

and Cu from the substrate. Table S1 gathers a summary of the peak positions and the corresponding planes and interplanar distances.

Detailed information about the wire-arrays composition was assessed by X-Ray Spectroscopies (see Supporting Information Section S3 and Methods). Figure S3 and S4 show the schematics of the scattering paths applied on the EXAFS analysis for FePc and FePcCl, correspondently. Figure S5 gathers the X-ray Absorption Spectroscopy (XAS) spectra for the FePc and FePcCl nanowires samples in comparison with their bulk crystalline counterparts. FePc and FePcCl bulk crystals present a pre-edge shoulder corresponding to a 1s → 3d transition from the Fe(II) and Fe(III) ions on square-planar configuration located at slightly different energies. These spectral features are ideal to identify the ion present on the sample. FePc nanowires XANES spectrum displays a similar pre-edge shoulder than the bulk crystalline FePc reference (Figure S6). Thus, we can conclude that the nanowires are composed of FePc stacked molecules. However, in the case of the FePcCl nanowires, the XANES shows two shoulders on the pre-edge region. The first shoulder coming from the expected Fe(III) ions (as shown in the bulk crystalline FePcCl reference) and a second component that can be attributed to Fe(II) ions. A rough estimation of the Fe(III)/Fe(II) ratio from these spectra was over 60-70%. Thus, there is very likely that a percentage of the original FePcCl precursor molecules were transformed to FePc during the nanowires deposition and/or characterization. EXAFS spectrum of the FePc nanowires (Figures 2 e), S7 and S8) were analysed by using a model that started from the known positions of the FePc atoms from the literature,[33,34] and then added contributions from the neighbouring molecules on the vertical stack. On this regard, the positions of these molecules were allowed to slightly shift horizontally, as is expected from the typical crystalline structures of phthalocyanines.[35] The Fe-Fe distance was fitted to be 0.384 nm, and the stacking molecules

were horizontally shifted by 0.080 nm. This result agrees with the previously shown SAED measurements. Figure 2 e) (left) shows the imaginary part and the magnitude of the Fourier Transform of the EXAFS signal of the FePc nanowires, giving a quite accurate fit up to 4.2 Å. The fit also shows a few interesting additional results which are described on the Supporting Information Section S3 along with the full details of the analysis. The EXAFS spectrum from the FePcCl nanowires was more complicated to analyse due to the mixture of both FePc and FePcCl local environments. In order to reduce the number of variables in the fitting procedure, we took the results from the EXAFS analysis of the FePc nanowire and maintained these values as fixed. Then we added a variable that accounts for the FePc/FePcCl ratio, and developed a model of the FePcCl local environment with its neighbouring molecules, similar to the above one (see details in SI). In the model, these neighbours would be stacked with Cl atoms positioned between them. Thus, each Fe ion will have a coordination shell with two Cl atoms. The results show that the Cl atoms stand at 0.229 nm of the Fe ions, and the neighbour Fe is located at 0.458 nm. These results are also in agreement with the SAED measurements. The FePc/FePcCl ratio was fixed to 30:70 for the fitting as determined from the XANES analysis. We were not able to quantify the horizontal shift of the stack, as the backscattering signal of the neighbour molecules N atoms is not strong enough to be analysed. Figure 2 e) (right) shows the imaginary part and the magnitude of the Fourier Transform of the EXAFS signal of the FePcCl, and its corresponding fit. Note this fit is not as accurate as the previous case due to the complex mixture we were considering in the model, so a relatively large error (~10%) was assumed on the quantitative results.

In order to further elucidate the chemical composition of the FePcCl NWs we carried out the characterization by UV-VIS-NIR transmission and XPS in high-density arrays and by EDX on individual FePcCl wires. Figure 3 a) shows the UV-VIS-NIR transmission spectra of FePc and

FePcCl solid powder and supported nanowires. The spectra of the FePc samples are characteristic of metallated phthalocyanines consisting in an intense Q band over 720 nm and a high energy B band over 340 nm. The spectra of the FePcCl samples present similar bands shifted to higher energies at over 672 nm (Q band) and over 335 nm (B band) with an additional absorption band at 854 nm. The samples are transparent in the NIR regions. In both cases the spectra of powder and supported nanowires samples are very similar being the supported powder and single crystalline films' spectral features located in the same spectral positions. However, the FePcCl sample presents a low energy shoulder in the position of the FePc Q absorption band that could indicate a minor FePc contribution.

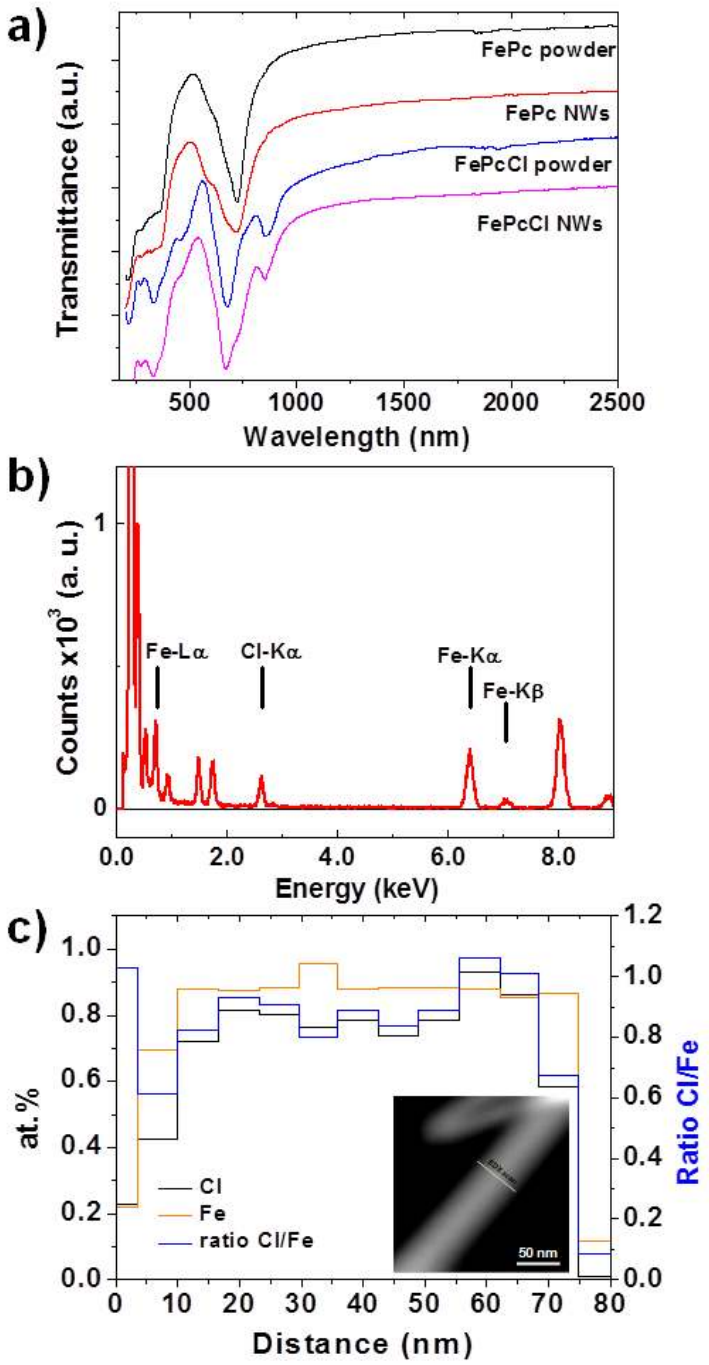

Figure 3. (a) UV-Vis-NIR spectra of the FePc and FePcCl supported powders and NWs grown on a TiO_2 thin film previously deposited on fused silica. The spectra have been displaced vertically with respect to one another for clarity. (b) EDX spectrum of a FePcCl nanowire obtained in the transmission electron microscope. The spectrum shows the relevant fluorescence

peaks used to calculate the Fe/Cl ratio. (c) Atomic percentage obtained for Cl and Fe signals, along to the estimated Cl/Fe ratio. Inset) STEM image indicating the EDX linear scanning for the FePcCl nanowire.

Figure 3 b) shows the EDX spectra corresponding to a FePcCl nanowire acquired in the TEM. Cl fluorescence peaks can be easily determined along with those of Fe and light elements. Cu and Al signals from the substrate seeds are also present. We estimated the composition along the cross section of the NW by a high resolution linear EDX scan (see Figure 3 c). The EDX results indicate a slight deficit of Cl in the external face of the NW reaching a constant value in the NW central region of Cl/Fe ~ 0.82. On the other hand, a high nanowire density FePcCl sample was characterized by XPS. A quantitative measurement of the Fe2p and Cl2p photoelectron peaks (Figure S9 and Table S6 in the Supporting Information) signals allowed calculating the Cl/Fe ratio to be over 0.93 by this technique. This value is quite close to the expected 1:1 ratio corresponding to the FePcCl molecular formula. Note that the surface sensitivity of the XPS enhances the detection of the molecules located at the sample surface. However, the determined ratio confirms, in good agreement with the EDX results, that only very minor percentage of the surface FePcCl molecules in the nanowires have indeed transformed into FePc.

Results gathered in Figures 1 to 3 and S2 to S9 indicate that both, FePc and FePcCl NWs are formed by a crystallization process with Cl atoms occupying a central position between two Fe(III) phthalocyanine molecules in the vertical molecular stacks in the case of the FePcCl NWs.

For the magnetization measurements, it is necessary to discern between the in-plane and out-of-plane directions respect to the phthalocyanine planes, as the exchange interaction should appear mostly on the out-of-plane direction. However, as shown in Figure 1, the phthalocyanine

self-assembled supported nanowires do not grow perpendicularly to the substrate and are bent[14,19] forming a randomly distributed mesh. Indeed, alignment and patterning of organic nanowires and nanofibers has become a ubiquitous issue in the topic as critical to prompt the integration of these nanostructures within spintronic and optoelectronic devices. Literature gathers approaches such as soft-printing lithography, template formation or seed-mediated orientation of the ONWs.[12,36-39] In this article, we take advantage of a recently developed method consisting in the alignment of the ONWs driven by electrostatic interaction with the plasma-sheath electric field.[19,21,28] The protocol involves the formation of an inorganic shell that acts as a scaffold that maintains the vertical orientation of the ONWs once the plasma is switched off. In practice, the FePcCl and FePc ONWs reach vertical alignment by growing by PECVD[40] a SiO_2 conformal shell. Figure 1c) shows the cross-sectional view and detail of an array of FePcCl nanowires coated with SiO_2. The coating is completely conformal, being thicker at the tip of the wires because of a self-shadowing effect enhanced by the vertical alignment.[19,28,41] Concretely, we have deposited a SiO_2 shell with a nominal thickness of 250 nm (i.e., the thickness measured by SEM of a thin film deposited under the same conditions and time). This value corresponds to the thickness of the shell on the top of the NWs. Because the self-shadowing effect, the thickness of the shell along the NWs length is smaller, in the order of 40 nm (see the HREM image in Figure 1 c-right). The straightening and preferential vertical alignment is clearly evidenced in the SEM micrographs showing that most of these hybrid nanowires are oriented perpendicularly to the substrate. Surface roughness of the shell and porous globular microstructure (see Figure 1 c) are in good agreement with the corresponding thin film counterpart deposited on flat substrates.[40] It is worth to stress that this shell acts solely as a mechanical or geometrical scaffold with not interference in the magnetic properties. Hence,

as it is proved in the HREM image of a FePcCl NW cover by the SiO_2 shell (Figure 1 c-right) the plasma deposition method provides the formation of the inorganic shell with no damage of the delicate organic nanowire single-crystalline structure. Figure 4 a) shows the magnetisation hysteresis loops at 5 K corresponding to the vertically aligned SiO_2-coated FePc nanowires, taken at both in-plane and out-of-plane geometry. We observe that the out-of-plane magnetisation direction presents some ferromagnetism, although with a small remanence and weak coercivity. On the in-plane direction, the system seems to follow a ferromagnetic behaviour as well, but with smaller remanence and coercivity. Figure 4 b) displays the hysteresis loop of the SiO_2-coated FePcCl nanowires. Again, ferromagnetism is found in both the out-of-plane and in-plane magnetisation directions, being also higher in the former case. Besides, the observed hysteresis loops in both directions are noticeably wider than those of FePc. The ferromagnetic behaviour is further evidenced in Figure 4 c), where the magnetisation in the out-of-plane directions for both samples at 0.1 T is plotted against temperature. Here we can see that both magnetisations follow the ferromagnetic characteristic shape, with a Curie temperature around 30 K.

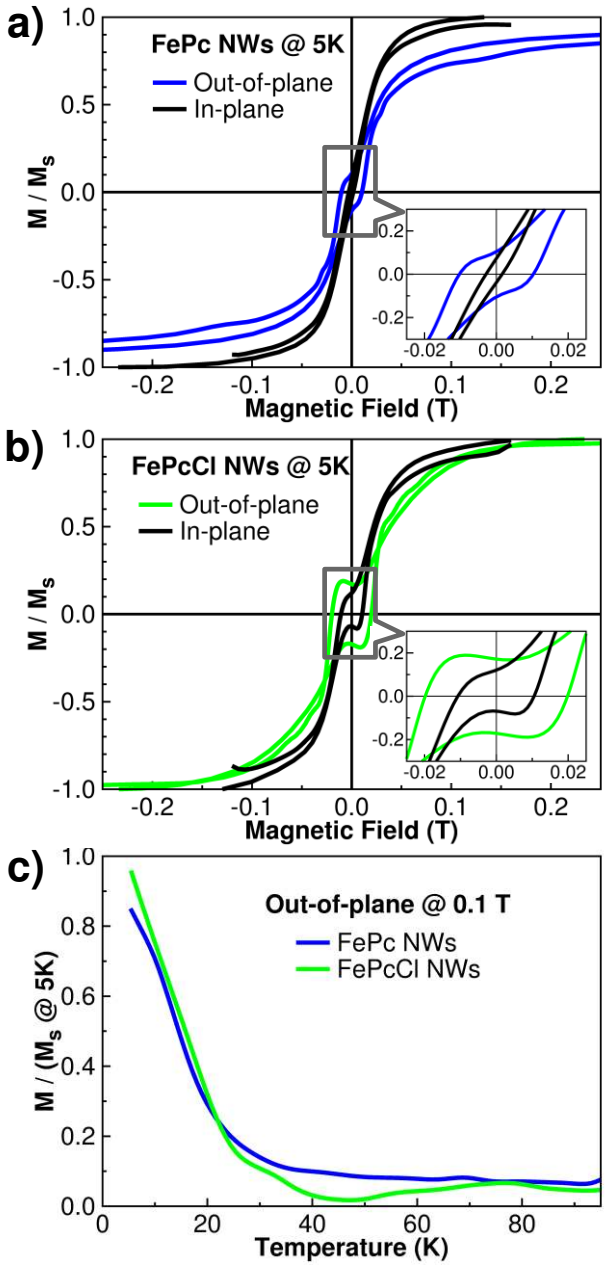

Figure 4: SQUID magnetization measurements, giving the hysteresis loops of vertically aligned SiO_2 coated supported nanowires of (a) FePc and (b) FePcCl at both out-of-plane and in-plane directions with respect to the substrate surface. The curves show the nanowires are ferromagnetic presenting an evident anisotropy. The insets show a zoom on the central region (c) Magnetisation

against temperature of the out-of-plane direction of SiO_2-coated supported nanowires of (a) FePc and (b) FePcCl. The Curie temperature is approximately 30K for both samples.

From these results, we can conclude that the vertical stacking of both molecules results in a noticeable anisotropy, with an easy axis perpendicular to the plane of the phthalocyanines, as expected due to their extremely anisotropic structure. Comparing both molecules, FePcCl presents wider hysteresis in both directions, which means that the higher spin state of the Fe(III) ion overcomes the interposition of the Cl atom. This type of interaction between Fe ions too far away from each other to be connected by direct exchange and is mediated by a diamagnetic material (i.e. the Cl ions) is named superexchange interaction[42] and is due to the extension of the Fe(III) wavefunction out over the Cl anion producing and orbital overlap. However, the exact nature of the superexchange interaction between the Fe ions according to the Goodenough-Kanamori-Anderson rules[43] would need a complete description of the molecular orbitals of the stacked FePc and FePcCl molecules, which is out of the scope of this paper.

Conclusions

In this work, we have presented the experimental conditions to synthesize single-crystalline supported nanowires by the physical vapour deposition of the non-planar Fe (III) phthalocyanine chloride molecule. We demonstrated that FePcCl NWs grow under controlled vacuum and substrate temperature conditions onto Si(100) coated with nanostructured Al, Cu or TiO_2 films. The FePcCl samples presented a high NW density, high aspect ratio, uniform cross-sections and lengths. A minor percentage of reduced Fe(II) was detected located at the nanowire surface.

The structural and magnetic properties of the FePcCl nanowires were compared with Fe(II)-phthalocyanine nanowires deposited by the same methodology to be used as reference. Structural and chemical characterization indicate the growth following a crystallization process of single-crystalline organic nanowires by the self-assembly of the non-planar FePcCl plausibly directed by a molecular stacking in which each Cl atom is shared sandwiched between two adjacent Fe (III) cations in two phthalocyanine macrocycles.

Once developed the synthetic route for the supported FePcCl nanowires, we studied the magnetic properties of the FePc and FePcCl nanowires after aligning them perpendicularly to the substrate by the plasma assisted deposition of a SiO_2 shell. The results indicate the vertically aligned FePcCl nanowires are ferromagnetic below 30K presenting a magnetic anisotropy on the direction perpendicular to the phthalocyanine planes in the single crystals due to a superexchange interaction between the Fe(III) cations. We trust this work will open new routes for the development, enhancing and controlling of the magnetism of oriented nanowire structures by the self-assembly of non-planar conjugated molecules and provides an unprecedented route

for the exploitation of the magnetic properties of organic 1D nanostructures in molecular electronics and spintronics.[45-49]

Methods. *Supported Organic Nanowires Formation.* FePc and FePcCl powders (Aldrich) were sublimated in a vacuum chamber from a low temperature effusion cell prepared for organic compounds evaporation. The molecular structures are shown in Figure 1. The base pressure of the chamber was below than 10^{-6} mbar. Ar gas was introduced into the reactor to obtain a working pressure of 0.02 mbar during the deposition using a calibrated mass flow controller (MKS). The distance from the cell to the sample holder was ~ 6.5 cm. For FePc, the temperature of the evaporation cell was adjusted to obtain a constant growth rate of around 0.4 Å. This rate was measured by a quartz microbalance calibrated to a density of 0.5 g/cm^3. The microbalance was located close to the sample holder and at the same distance from the evaporation cell. The temperature of the sample holder was kept around 220ºC during the deposition to favour the formation of the nanowires.[14] Similarly, for FePcCl the growth rate was adjusted to 0.45 Å/s and the sample holder was kept at 210ºC.

Substrates. Substrates with suitable seeds needed for the synthesis were prepared and used for the nanowire deposition. For this, Si(100) wafers and fused silica slides were coated in three ways: a) with Al by thermal evaporation in high vacuum, b) with Cu by oblique angle deposition (OAD)[44] and c) with a thin layer of mesoporous TiO_2 deposited by PECVD.[21] These methods yielded nanostructured films or nanoparticles with mean size in the range of 100 nm when the thickness was settled below the percolation limit. These systems served as nucleation centers for the preferential condensation of the molecule. Polycrystalline FePc and FePcCl films were formed under the same experimental conditions on pristine substrates. These latter samples were utilized as references to perform optical absorption measurements.

SiO_2 shell formation. A conformal SiO_2 shell was formed by plasma-enhanced chemical vapour deposition (PECVD), using a microwave (2.45 MHz) ERC reactor in a downstream configuration keeping the substrates at room temperature.[19,21] The precursor (chlorotrimethylsilane, Sigma-Aldrich) was introduced into the chamber through a heated dosing line using a mass flow controller. The microwave plasma source (SLAN, Plasma Consult GmbH) was coupled to the reaction chamber and separated from it by a grounded grid located 10 cm above the sample holder and operated at 600 W. The working gas was 1×10^{-2} mbar of 100% O_2.

Materials Characterization. Scanning electron microscopy (SEM) planar and cross-sectional views images were taken with a Hitachi S4800 field emission SEM microscope. Analyses of the SEM images were carried out using the free available ImageJ software (https://imagej.nih.gov/ij). Selected Area Electron Diffraction (SAED) patterns were carried out in a Philips CM200 transmission electron microscope (TEM). High resolution TEM images were registered in a FEI-Tecnai G2F30 field emission scanning TEM (STEM-FEG) equipped with a S-Twin objective lens and operating at 80KV. The TEM analyses let us to determine both the column spacing between the molecules on a single nanowire and the inter-molecular spacing and relative orientation of the characteristic herring-bone structure resulting from the molecular self-assembly.[15] The nanowires were scraped from the Al/Si(100) substrates and deposited on gold grids for the TEM analysis. Energy-dispersive X ray (EDX) spectra were recorded during the TEM measurements estimate the Fe/Cl ratio EDX profiles were acquired with a FEI Tecnai Osiris TEM/STEM 80-200 working at 200 kV. Post-processing of EDX data was performed with the open source Hyperspy software: hyperspy.org. as described elsewhere.[45] X-ray absorption spectra at the Fe K edge in fluorescence mode were recorded at the SAMBA beamline of the

SOLEIL Synchrotron. The objectives of these measurements were: a) to determine the atomic distances on the local environments of the Fe ions in both the FePc and FePcCl nanowires and crystalline reference samples and b) to quantify the vertical Fe-Fe separation on the nanowire stacking. UV-Vis-NIR transmission spectra were collected in a PerkinElmer Lambda 750 UV/Vis/NIR spectrophotometer. XPS measurements of the FePcCl nanowire sample were obtained using a Phoibos 100 DLD X-ray spectrometer from SPECS working in the pass energy constant mode and using the Mg Kα as excitation source. Superconducting quantum interference device (SQUID) magnetometry was used to measure the samples' magnetisation. Hysteresis curves were recorded at low temperature (5K) to ensure the maximum magnetisation. The temperature behaviour of the magnetisation at 0.1 T of external field was taken from 5 to 100K to check for the ferromagnetic character of the samples and estimate the Curie temperature. The measurements were made at both in-plane and out-of-plane directions (referring to the substrate surface) to investigate the expected magnetic anisotropy caused by the structural anisotropy.

ASSOCIATED CONTENT

Supporting Information. Statistics on the NWs thickness. Schematic on the nanowires assembly, additional XRD pattern and X-Ray Spectroscopy results are included in this section.

Filippin_et_al_SupportingInformation (PDF)

AUTHOR INFORMATION

***victor.lopez@csic.es, anaisabel.borras@icmse.csic.es**

Author Contributions

The manuscript was written through contributions of all authors. All authors have given approval to the final version of the manuscript.

ACKNOWLEDGMENT

We thank the EU/FEDER and MINECO-AEI for financial support (Projects MAT2013-42900-P, MAT2016-79866-R), the EU/Junta de Andalucía Talent-Hub Program and the EU (Grant Agreement 312483 - ESTEEM2 (Integrated Infrastructure Initiative-I3), (FP/2007-2013)/ERC Grant Agreement 291522 - 3DIMAGE, Grant Number REGPOT-CT-2011-285895-Al-NANOFUNC). JRS-V and AngelB acknowledge funding from EU project *PlasmaPerovSol*. This project has received funding from the European Union's Horizon 2020 research and innovation programme under the Marie Skłodowska-Curie grant agreement No 661480.

REFERENCES

[1] Dasgupta, N. P.; Sun, J.; Liu, C.; Brittman, S.; Andrews, S. C.; Lim, J.; Gao, H.; Yan, R.; Yang P. 25th Anniversary Article: Semiconductor Nanowires – Synthesis, Characterization, and Applications. *Adv. Mater.* **2014**, *26*, 2137-2184.

[2] Briseno, A. L.; Mannsfeld, S. C. B.; Jenekhe, S. A.; Bao, Z.; Xia, Y. Introducing Organic Nanowire Transistors. *Mater. Today* **2008**, *11*, 38-47.

[3] Zang, L.; Che, Y.; Moore, J. S. One-Dimensional Self-Assembly of Planar pi-Conjugated Molecules: Adaptable Building Blocks for Organic Nanodevices. *Acc. Chem. Res.* **2008**, *41*, 1596-1608.

[4] Zhao, Y. S.; Fu, H. B.; Hu, F. Q.; Peng, A. D.; Yang, W. S.; Yao, J. N. Tunable Emission from Binary Organic One-Dimensional Nanomaterials: An alternative approach to white-light emission. *Adv. Mater.* **2008**, *20*, 79-83.

[5] Walther, A.; Yuan, J.; Abetz, V.; Mueller, A. H. E. Structure-Tunable Bidirectional Hybrid Nanowires via Multicompartment Cylinders. *Nano Lett.* **2009**, *9*, 2026-2030.

[6] Guo, Y.; Xu, L.; Liu, H.; Li, Y.; Che, C. M.; Li, Y. Self-Assembly of Functional Molecules into 1D Crystalline Nanostructures. *Adv. Mater.* **2015**, *27*, 985–1013.

[7] Cui, Q. H.; Jiang, L.; Zhang, C.; Zhao, Y. S.; Hu, W.; Yao, J. Coaxial Organic p-n Heterojunction Nanowire Arrays: One-Step Synthesis and Photoelectric Properties. *Adv. Mater.* **2012**, *24*, 2332–2336.

[8] Shaymurat, T.; Tang, Q.; Tong, Y.; Dong, L.; Liu, Y. Gas Dielectric Transistor of CuPc Single Crystalline Nanowire for SO2 Detection Down to Sub-ppm Levels at Room Temperature. *Adv. Mater.* **2013**, *25*, 2269–2273.

[9] Zhang, W.; Yan, Y.; Gu, J.; Yao, J.; Zhao, J. S. Low-Threshold Wavelength-Switchable Organic Nanowire Lasers Based on Excited-State Intramolecular Proton Transfer. *Angew. Chem. Int. Ed.* **2015**, *54*, 7125 – 7129.

[10] Zheng, J. Y.; Xu, H.; Wang, J.; Winters, S.; Motta, C.; Karademir, E.; Zhu, W.; Varrla, E.; Duesberg, G. S.; Sanvito, S.; Hu, W.; Donegan, J. F. Vertical Single-Crystalline Organic Nanowires on Graphene: Solution-Phase Epitaxy and Optical Microcavities. *Nano Lett.* **2016**, *16*, 4754−4762.

[11] Borras, A.; Gröning, O.; Köble, J.; Gröning, P. Connecting Organic Nanowires. *Adv. Mater.* **2009**, *21*, 4816–4819.

[12] Borras, A.; Gröning, P.; Sanchez-Valencia, J. R.; Barranco, A.; Espinos, J. P.; Gonzalez-Elipe, A. R. Air- and Light-Stable Superhydrophobic Colored Surfaces Based on Supported Organic Nanowires. *Langmuir* **2010**, *26*, 1487–1492.

[13] Deng, W.; Zhang, X.; Wang, L.; Wang, J.; Shang, Q.; Zhang, X.; Huang, L.; Jie, J. Wafer-Scale Precise Patterning of Organic Single-Crystal Nanowire Arrays via a Photolithography-Assisted Spin-Coating Method. *Adv. Mater.* **2015**, *27*, 7305–7312.

[14] Borras, A.; Aguirre, M.; Gröening, O.; Lopez-Cartes, C.; Gröning, P. Synthesis of Supported Single-Crystalline Organic Nanowires by Physical Vapor Deposition. *Chem. Mater.* **2008**, *20*, 7371–7373.

[15] Borras, A.; Gröning, O.; Aguirre, M.; Gramm, F.; Gröning, P. One-Step Dry Method for the Synthesis of Supported Single-Crystalline Organic Nanowires Formed by π-Conjugated Molecules. *Langmuir* **2010**, *26*, 5763–5771.

[16] Mbenkum, B.N.; Barrena, E.; Zhang, X.; Kelsch, M.; Dosch, H. Selective Growth of Organic 1-D Structures on Au Nanoparticle Arrays. *Nano Lett.* **2006**, *6*, 2852-2855.

[17] Lokesh, K. S.; Keersmaecker, M.; Adriaens, A. Self-Assembled Films of Porphyrins with Amine Groups at Different Positions: Influence of Their Orientation on the Corrosion Inhibition and the Electrocatalytic Activity. *Molecules* **2012**, *17*, 7824-7842.

[18] Alcaire, M.; Sanchez-Valencia, J. R.; Aparicio, F. J.; Saghi, Z.; Gonzalez-Gonzalez, J. C.; Barranco, A.; Zian, Y. O.; Gonzalez-Elipe, A. R.; Midgley, P.; Espinos, J. P.; Gröning, P.;

Borras, A. Soft Plasma Processing of Organic Nanowires: A Route for the Fabrication of 1d Organic Heterostructures and the Template Synthesis of Inorganic 1D Nanostructures. *Nanoscale* **2011**, *3*, 4554–4559.

[19] Macias-Montero, M.; Filippin, A. N.; Saghi, Z.; Aparicio, F. J.; Barranco, A.; Espinos, J. P.; Frutos, F.; Gonzalez-Elipe, A. R.; Borras, A. Vertically Aligned Hybrid Core/Shell Semiconductor Nanowires for Photonics Applications. *Advanced Functional Materials* **2013**, *23,* 5981–5989

[20] Oulad-Zian, Y.; Sanchez-Valencia, J. R.; Parra-Barranco, J.; Hamad, S.; Espinos, J. P.; Barranco, A.; Ferrer, J.; Coll, M.; Borras, A. Ultraviolet Pretreatment of Titanium Dioxide and Tin-Doped Indium Oxide Surfaces as a Promoter of the Adsorption of Organic Molecules in Dry Deposition Processes: Light Patterning of Organic Nanowires. *Langmuir* **2015**, *31*, 8294-8302.

[21] Filippin, A. N.; Macias-Montero, M.; Saghi, Z.; Idigoras, J.; Burdet, P.; Barranco, A.; Midgley, P.; Anta, J. A.; Borras, A. Vacuum Template Synthesis of Multifunctional Nanotubes with Tailored Nanostructured Walls. *Sci. Rep.* **2016**, *6*, 20637.

[22] Bartolome, J. S.; Luis, F.; Fernandez, J. F.; Molecular Magnets: Physics and Applications, Springer (**2014**) ISSSN 1434-4904.

[23] Bartolome, J. S.; Bartolome, F.; Garcia, L. M.; Filoti, G.; Gredig, T.; Colesniuc, C. N.; Shuller, I. K.; Cezar, J. C. Highly Unquenched Orbital Moment in Textured Fe-Phthalocyanine Thin Films. *Phys. Rev. B* **2010**, *81*, 195405.

[24] Papageorgiou, N.; Salomon, E.; Angot, T.; Layet, J. M.; Giovanelli, L.; Le Lay, G. Physics of Ultra-Thin Phthalocyanine Films on Semiconductors. *Prog. Surf. Sci.* **2004**, *77*, 139–170.

[25] Yoshizawa, S.; Minamitani, E.; Vijayaraghavan, S.; Mishra, P.; Takagi, Y.; Yokoyama, T.; Oba, H.; Nitta, J.; Sakamoto, K.; Watanabe, S.; Nakayama, T.; Takashi, U. Controlled Modification of Superconductivity in Epitaxial Atomic Layer-Organic Molecule Heterostructures. *Nano Lett.* **2017**, *17*, 2287-2293.

[26] Wende, H.; Bernien, M.; Luo, J.; Sorg, C.; Ponpandian, N.; Kurde, J.; Miguel, J.; Piantek, M.; Xu, X.; Eckhold, Ph.; Kuch, W.; Baberschke, K.; Panchmatia, P. M.; Sanyal, B.; Oppeneer, P. M.; Eriksson, O. Substrate-Induced Magnetic Ordering and Switching of Iron Porphyrin Molecules. *Nature Mater.* **2007**, *6*, 516–520.

[27] Gredig, T.; Colesniuc, C. N.; Crooker, S. A.; Schuller, I. K. Substrate-Controlled Ferromagnetism in Iron Phthalocyanine Films Due to One-Dimensional Iron Chains. *Phys. Rev. B* **2012**, *86*, 014409.

[28] Filippin, A. N.; Sanchez-Valencia, J. R.; Idigoras, J.; Rojas, T. C.; Barranco, A.; Anta, J. A.; Borras, A. Plasma Assisted Deposition of Single and Multistacked TiO_2 Hierarchical Nanotube Photoanodes. *Nanoscale* **2017**, *9*, 8133-8141.

[29] Haynes, W. M. (Ed). CRC Handbook of Chemistry and Physics, 97th Edition, **2016.**

[30] Tong, W. Y.; Djurisic, A. B.; Xie, M. H.; Ng, A. C. M.; Cheung, K. Y.; Chan, W. K.; Leung, Y. H.; Lin, H. W.; Gwo, S. Metal Phthalocyanine Nanoribbons and Nanowires. *J. Phys. Chem. B* **2006**, *110*, 17406-17413.

[31] Wang, H.; Mauthoor, S.; Din, S.; Gardener, J. A.; Chang, R.; Warner, M.; Aeppli, G.; McComb, D. W.; Ryan, M. P.; Wu, W.; Fisher, A. J.; Stoneham, M.; Heutz, S. Ultralong Copper Phthalocyanine Nanowires with New Crystal Structure and Broad Optical Absorption. *ACS Nano* **2010**, *4*, 3921-3926.

[32] Berger, O.; Fischer, W. J.; Adolphi, B.; Tierbach, S.; Melev, V.; Schereiber, J. Studies on Phase Transformations of Cu-Phthalocyanine Thin Films. *J. Mater. Sci.* **2000**, *11*, 331.

[33] Carrera, F.; Sanchez-Marcos, E.; Merkling, P. J.; Chaboy, J.; Munoz-Paez, A. Nature of Metal Binding Sites in Cu (II) Complexes with Histidine and Related N-Coordinating Ligands, as Studied by EXAFS. *Inorg. Chem.* **2004**, *43*, 7185–7193.

[34] Liao, M. S.; Scheiner, S. Electronic Structure and Bonding in Metal Phthalocyanines, Metal=Fe, Co, Ni, Cu, Zn, Mg. *J. Chem. Phys.* **2001**, *114*, 9780-9791.

[35] Hoshino, A. Redetermination of the Crystal Structure of α-Copper Phthalocyanine Grown on KCl. *Acta Cryst.* **2003**, *B59*, 393–403.

[36] Min, S. Y.; Kim, T. S.; Lee, Y.; Cho, H.; Xu, W.; Lee, T. W. Organic Nanowire Fabrication and Device Applications. Small **2015**, *11*, 45-62.

[37] Park, K. S.; Cho, B.; Baek, J.; Hwang, J. K.; Lee, H.; Sung, M. M. Single-Crystal Organic Nanowire Electronics by Direct Printing from Molecular Solutions *Adv. Funct. Mater.* 2013, *23*, 4776-4784.

[38] Wu, Y.; Zhang, X.; Pan, H.; Zhang, X.; Zhang, Y.; Zhang, X.; Jie, J. Large-Area Aligned Growth of Single-Crystalline Organic Nanowire Arrays for High-Performance Photodetectors. *Nanotechnol.* **2013**, *24*, 355201.

[39] Hu, Z.; Muls, B.; Gence, L.; Serban, D. A.; Hofkens, J.; Melinte, S.; Nysten, B.; Demoustier-Champagne, S.; Jonas, A. M. High-Throughput Fabrication of Organic Nanowire Devices with Preferential Internal Alignment and Improved Performance. *Nano Lett.* **2007***, 7*, 3639-3644.

[40] Barranco, A.; Cotrino, J.; Yubero, F.; Espinós, J. P.; Benítez, J.; Clerc, C.; González-Elipe, A. R. Synthesis of SiO_2 and $SiO_xC_yH_z$ Thin Films by Microwave Plasma CVD. *Thin Solid Films* **2001**, *401*, 150-158.

[41] Moore, K.; Clemons, C. B.; Kreider, K. L.; Young, G. W. Modeling and Simulation of Axisymmetric Coating Growth on Nanofibers. *J. Appl. Phys.* **2007**, *101*, 064305.

[42] Lalena, J. N.; Cleary, D. A. Principles of Inorganic Materials Design. John Wiley & Sons, **2010**.

[43] Furdyna, J. K.; Samarth, N. Magnetic Properties of Diluted Magnetic Semiconductors: A Review. *J. Appl. Phys.* **1987**, *61*, 3526-3531

[44] Barranco, A.; Borras, A.; Gonzalez-Elipe, A. R.; Palmero, A. Perspectives on Oblique Angle Deposition of Thin Films: from Fundamentals to Devices. *Prog. Mater. Sci.* **2016**, 76, 59-153.

[45] Burdet, P.; Saghi, Z.; Filippin, A. N.; Borras, A.; Midgley, P. A. A Novel 3D Absorption Correction Method for Quantitative EDX-STEM Tomography. *Ultramicroscopy* **2016**, *160*, 118-129.

[46] Sanvito, S. Molecular Spintronics. *Chem. Soc. Rev.* **2011**, *40*, 3336-3355.

[47] Sanvito, S.; Dediu, V. A. Spintronics: News from the Organic Arena. *Nature Nanotechnology* **2012**, *7*, 696-697.

[48] Kuang, G.; Zhang, Q.; Lin, T.; Pang, R.; Shi, X.; Xu, H.; Lin, N. Mechanically-Controlled Reversible Spin Crossover of Single Fe-Porphyrin Molecules. ACS Nano **2017**, *11*, 6295-6300

[49] Sierda, E.; Abadia, M.; Brede, J.; Elsebach, M.; Bugenhagen, B.; Prosenc, M. H.; Bazarnik, M.; Wiesendanger, R. On-Surface Oligomerization of Self-Terminating Molecular Chains for the Design of Spintronic Devices. *ACS Nano* **2017**, *11*, 9200-9206.